

ine ecosystems are commonly sustained by groundwater inflows at those times (Kløve et al., 2011; Barron et al., 2012; Cartwright and Gilfedder, 2015). Thus, understanding the distribution and magnitude of groundwater inflows is important for managing and protecting these commonly vulnerable ecosystems. Failure to understand groundwater contributions to rivers may result in double allocation of water resources (i.e., the surface water and groundwater allocations might represent the same water). Documenting the distribution and quantity of groundwater inflows to rivers is also required for flood forecasting, understanding the impacts of contaminants on rivers, and understanding the potential impacts of climate or landuse changes on river systems.

There are many methods to assess the distribution and magnitude of groundwater inflows to rivers (e.g., Brodie et al., 2007). Differential gauging may be used to determine both groundwater inflows and outflows. In many catchments, however, the distribution of river gauges is insufficient to allow anything other than a large-scale categorisation of gaining and losing behaviour. Numerical techniques based on river hydrographs (e.g., Nathan and McMahon, 1990; Askoy et al., 2009) provide a straightforward method of estimating baseflow. However, these are of limited use in highly-regulated rivers and may aggregate several stores of water including regional groundwater, bank return flows, and interflow into the baseflow component (McCallum et al., 2012; Cartwright et al., 2014a). Groundwater flow models and water balance models may also be used to calculate groundwater inflows but their applicability requires a detailed knowledge of hydrological parameters such as hydraulic conductivity, groundwater elevations, evapotranspiration rates, and runoff.

Providing that groundwater and surface water have different concentrations of a given geochemical component, changes in the geochemistry of the river may be used to estimate groundwater inflows into individual reaches (e.g., Cook, 2013). Tracers such as major ions, stable isotopes, radioactive isotopes, and chlorofluorocarbons have been used to quantify groundwater inflows to rivers (e.g., Ellins et al., 1990; Genereux and Hemond, 1992; Négrel et al., 2001; Stellato et al., 2008; Cartwright et al., 2011; Cook, 2013; Bourke et al., 2014a, b). Geochemical tracers only quantify

9207

groundwater inflows, and while they are commonly used to determine the distribution of gaining and losing reaches, they do not quantify the magnitude of any groundwater outflows. Thus, if rivers have significant losing sections, the calculated groundwater inflows from geochemical tracers may exceed the total increase in streamflow.

1.1 ²²²Rn as a tracer of groundwater inflows

²²²Rn, which is an intermediate isotope in the ²³⁸U to ²⁰⁶Pb decay series, is an important tracer for quantifying groundwater inflows to rivers. ²²²Rn has a half-life of 3.8 days and the activity of ²²²Rn reaches secular equilibrium with its parent isotope ²²⁶Ra over 3 to 4 weeks (approximately 5 half-lives) (Cecil and Green, 2000). Because the concentrations of Ra in minerals are several orders of magnitude higher than dissolved Ra concentrations in surface water, groundwater ²²²Rn activities are commonly two or three orders of magnitude higher than those of surface water (Cecil and Green, 2000). This makes ²²²Rn a valuable tracer in catchments where the groundwater has similar major ion concentrations and stable isotope ratios to the river water. As ²²²Rn activities in rivers decline downstream from regions of groundwater inflow due to radioactive decay and degassing to the atmosphere (Ellins et al., 1990; Genereux and Hemond, 1992), ²²²Rn is also useful in determining locations of groundwater inflow, even if the inflows are not quantified.

Assuming that the atmosphere contains negligible radon, the change in ²²²Rn activities along a river may be estimated by mass balance:

$$Q \frac{dc_r}{dx} = I(c_{gw} - c_r) + wEc_r + F_h + F_p - kdwc_r - \lambda dwc_r \quad (1)$$

(modified from Mullinger et al., 2007; Cartwright et al., 2011; and Cook, 2013). In Eq. (1): Q is streamflow ($m^3 \text{ day}^{-1}$); I is the groundwater inflow ($m^3 m^{-1} \text{ day}^{-1}$); c_r and c_{gw} are the ²²²Rn activities ($Bq m^{-3}$) in the river and groundwater, respectively; E is the evaporation rate ($m \text{ day}^{-1}$); x is longitudinal distance (m); w is river width (m); d is river depth (m); F_h and F_p are the fluxes of ²²²Rn ($Bq m^{-1} \text{ day}^{-1}$) from the hyporheic

9208

zone and the broader parafluvial zone, respectively; k is the gas-transfer coefficient (day^{-1}); and λ is the decay constant (0.181 day^{-1}) (Table 1). Unlike most applications of ^{222}Rn mass balance, F_h and F_p have been separated which allows both small-scale (hyporheic) and larger-scale (parafluvial) flow through the near-river sediments to be considered (c.f., Bourke et al., 2014a). Equation (1) can also be used to estimate the changes in composition of major ion tracers. Since the concentration of a conservative tracer such as Cl is controlled only by groundwater inflows and evaporation, only the first two terms on the right-hand-side of Eq. (1) are relevant. If the river is solely fed by groundwater the increase in streamflow downstream is:

$$\frac{dQ}{dx} = I - EW. \quad (2)$$

Uncertainties in the parameters in Eq. (1) can result in significant uncertainties in calculated groundwater inflows. The evaporation term is generally much smaller than the other terms in Eq. (1), and thus uncertainties in evaporation rates have little impact on the calculations (Cartwright et al., 2011; Cook, 2013). By contrast, heterogeneous ^{222}Rn activities in groundwater may result in substantial uncertainties in calculated groundwater inflows (Cook et al., 2006; Mullinger et al., 2007; Unland et al., 2013; Yu et al., 2013; Cartwright et al., 2011; Atkinson et al., 2015); groundwater Cl concentrations are also commonly heterogeneous (Cook, 2013; Cartwright, 2014b) and this leads to similar uncertainties when using Cl to estimate groundwater inflows. Additionally, while it is well established that the rate of Rn degassing increases with increasing river turbulence and decreasing river depth, different empirical formulations that predict k from river widths, depths, and velocities can yield disparate k values (Genereux and Hemond, 1992), which can also lead to significant uncertainties in calculated groundwater inflows.

9209

1.2 Hyporheic and parafluvial flow

In most rivers, there is likely to be a contribution of ^{222}Rn resulting from water flowing through the hyporheic zone (the zone immediately below the river bed through which water flows driven by irregularities in the river bed) and the broader parafluvial zone, which includes features such as point bars and gravel banks (Boulton et al., 1998; Edwardson et al., 2003). Both hyporheic and parafluvial flow represent water that exfiltrates the river and subsequently re-infiltrates at some point downstream. The ^{222}Rn activity in water flowing through the hyporheic and parafluvial zones increases over time due to ^{222}Rn emanation from the sediments and the contribution of ^{222}Rn from these sources needs to be estimated when calculating groundwater inflows (Cook, 2013). While the contribution of ^{222}Rn derived from the hyporheic zone is commonly considered, few studies have considered the contribution of ^{222}Rn from the parafluvial zone (c.f. Bourke et al., 2014a; Cartwright et al., 2014b); however, in rivers with coarse-grained sediments on the floodplain the input of ^{222}Rn from the parafluvial zone may be significant.

The ^{222}Rn activity in the hyporheic or parafluvial zone waters (c_h or c_p) is governed by the ^{222}Rn activity of the water flowing into the hyporheic zone (c_{in}), the ^{222}Rn emanation rate (γ in $\text{Bq m}^{-3} \text{ day}^{-1}$), and the residence time (t_h or t_p , in days):

$$c_h = \left(\frac{\gamma}{\lambda} - c_{in} \right) \left(1 - e^{-\lambda t_h} \right) + c_{in} \quad (3)$$

(Hoehn et al., 1992; Hoehn and Cirpka, 2006) (Fig. 1a). c_h increases with residence time (t_h) and at steady state (i.e., as t_h in Eq. 3 $\rightarrow \infty$), $c_h = \gamma/\lambda$. In a losing or neutral (i.e. neither gaining nor losing) river $c_{in} = c_r$. In a gaining river, water derived from the river will mix in the alluvial sediments with upwelling regional groundwater that has high ^{222}Rn activities and Cartwright et al. (2014b) discussed using the concentration of a conservative ion such as Cl to estimate the degree of mixing within the alluvial sediments to estimate c_{in} . Assuming that all the water entering the hyporheic zone

9210

2 Local geology and hydrogeology

The Avon River occurs within the Gippsland Basin in southeast Australia (Fig. 2) and has a total catchment area of $\sim 1830 \text{ km}^2$ (Cochrane et al., 1991; Department of Environment and Primary Industries, 2015). The Avon River is unregulated and drains the southern slopes of the Victorian Alps (maximum elevation in the catchment is 1634 m), and discharges into Lake Wellington, which is a coastal saline lake connected to the Southern Ocean. The upper slopes represent $\sim 30\%$ of the Avon catchment and are dominated by temperate native eucalyptus forest while the majority of the plains representing $\sim 70\%$ of the catchment have been cleared for agriculture, including dairying, sheep grazing, and vegetable production. The estimated population of the Avon catchment is ~ 4000 with Stratford being the largest town (population ~ 2000).

The highlands of the Victorian Alps comprise indurated Palaeozoic and Mesozoic igneous rocks and metasediments that only host groundwater flow in fractures or in near-surface weathered zones (Walker and Mollica, 1990; Cochrane et al., 1991). These rocks form the basement to the Tertiary and Quaternary sediments of the Gippsland Basin (Fig. 2). The shallowest regional aquifer within the Avon Catchment is the Pliocene to Pleistocene Haunted Hill Formation which comprises up to 40 m of interbedded alluvial sands and clays that have hydraulic conductivities between 10^{-7} and 10^{-5} m s^{-1} (Brumley et al., 1981; Walker and Mollica, 1990). Quaternary sediments that consist of coarse-grained sand and gravels interbedded with finer-grained silts occur mainly within the river valleys and have hydraulic conductivities of 10^{-5} and 10^{-2} m s^{-1} (Brumley et al., 1981; Walker and Mollica, 1990).

Average rainfall within the Avon catchment ranges from $\sim 1.5 \text{ m yr}^{-1}$ in the highlands to $\sim 0.9 \text{ m yr}^{-1}$ on the plains and most precipitation occurs in the austral winter (June to September) (Bureau of Meteorology, 2015). The Avon River displays strong seasonal flows with $\sim 80\%$ of annual streamflow occurring during winter (Department of Environment and Primary Industries, 2015). This study focusses on the reaches of the Avon River located on the plains formed by the Gippsland Basin sediments that are

9213

upstream of tidal influence. Streamflow is measured at three sites (The Channel, Stratford, and Chinns Bridge: Fig. 2). Total annual streamflow at Stratford (Fig. 2) between 1977 and 2014 ranged from 1.3×10^7 to $9.02 \times 10^8 \text{ m}^3 \text{ yr}^{-1}$ (median = $3.04 \times 10^8 \text{ m}^3 \text{ yr}^{-1}$) and varies with total annual rainfall (Department of Environment and Primary Industries, 2015). The Avon River only ceases to flow during the summers of severe drought years (e.g., 1983) and experiences periodic floods during high rainfall periods (Fig. 3). Streamflow generally increases downstream at all flow conditions, except at very low flows when streamflow decreases between Stratford and Chinns Bridge. Valencia Creek and Freestone Creek are the main tributaries; both have streamflow measurements and both enter the Avon in the upper reaches of the studied section.

The Avon River has incised through the Haunted Hill Formation and Quaternary sediments to create terraces that are up to 30 m high with a lower floodplain that is up to 500 m wide. Where it crosses the sedimentary plains, the Avon River comprises a sequence of slow-flowing pools that are typically 10 to 30 m wide, up to 2 m deep at low flows, and up to 2 km long. These pools are connected by shorter (typically 10's to 100's m) and narrow (typically $< 5 \text{ m}$) faster-flowing riffle sections that commonly have steep longitudinal gradients.

The floodplain of the Avon River comprises numerous gravel banks and point bars of coarse-grained unconsolidated sediments with clasts of up to 50 cm in diameter. The coarse-grained alluvial sediments are most common between Browns and Redbank (Fig. 2); downstream of Redbank, the Avon River occupies an incised channel with steep banks of finer-grained (clay to sand sized) sediments. The alluvial sediments are sparsely vegetated and the geometry of the floodplain changes markedly following flood events, such as those in 2011, 2012, and 2013 (Fig. 3). These changes include the downstream migration of pools (often by several tens of metres), scouring of the alluvial sediments, and changes to the size and location of the sediment banks. In regions where the river is incised, there are seeps of water at the base of the slope and permanent patches of vegetation such as *Juncus* that commonly colonise waterlogged soils in Australia.

9214

Groundwater flows from the Victorian Alps to the coast (Hofmann and Cartwright, 2013: Fig. 2); however, there are few groundwater monitoring bores in the Avon catchment that can be used to construct detailed groundwater flow paths or define the relationship of the Avon River to the groundwater. Both the Avon River and shallow groundwater from the Haunted Hills and Quaternary aquifers are used for irrigation and stock use, and groundwater is also used for water supply for Briagolong (population ~ 950) (Gippsland Water, 2012). Current annual groundwater allocations are $1.4 \times 10^7 \text{ m}^3$, although these are not fully utilised at present (Gippsland Water, 2012). Use of water from the Avon River and its tributaries for irrigation is up to $8 \times 10^6 \text{ m}^3 \text{ yr}^{-1}$ (~ 2.6 % of the annual median streamflow at Stratford); however, this is seasonally adjusted with a prohibition on river water use when the streamflow at Stratford is $< 10^4 \text{ m}^3 \text{ day}^{-1}$.

The incised nature of the Avon River and the fact that it rarely ceases to flow has led to an assumption that it receives significant groundwater inflows (Gippsland Water, 2012); however, there has been little attempt to quantify the inflows or determine their distribution. Such information is required to protect and manage the Avon River, especially in assessing the potential impacts of increased groundwater or surface water use.

3 Methods

Sampling took place between February 2009 and February 2015 in six sampling campaigns. The sampling periods (Fig. 3a) include periods of very low streamflow (February 2009 and March 2014), periods of low to moderate streamflow (April 2010 and February 2015), and periods of higher streamflow (September 2010, and July 2014). Major flood events between 2011 and 2013 caused redistribution of the pools and sediment banks in the river. Each sampling campaign involved sampling the river sites (Table S1, Fig. 2) over a two to three day period, with the February 2015 sampling campaign involving additional sites to the others. Streamflow data is from gauging stations at The Channel, Stratford, and Chinnns Bridge on the Avon River and from gauges

9215

on the Valencia Creek and Freestone Creek tributaries (Department of Environment and Primary Industries, 2015: Fig. 2). Distances are measured relative to the first site at Browns (Fig. 1)

Sampling and analytical techniques were similar to those in other studies (e.g. Unland et al., 2013; Yu et al., 2013; Cartwright et al., 2014b). River samples were collected from 0.5–1 m below the river surface using a manual collector mounted on a pole. Groundwater was sampled from bores installed on the river bank and floodplain at Stratford and Pearces Lane (Fig. 2) that have 1 to 3 m long screens. Water was extracted using an impeller pump set at the screened interval and at least 3 bore volumes of water were purged before sampling. Cations (Tables S1 and S2) were analysed on samples that had been filtered through $0.45 \mu\text{m}$ cellulose nitrate filters and acidified to $\text{pH} < 2$ using a ThermoFinnigan quadrupole ICP-MS at Monash University. Anions (Tables S1 and S2) were analysed on filtered unacidified samples using a Metrohm ion chromatograph at Monash University. The precision of major ion concentrations based on replicate analyses is 2–5 %. A suite of anions and cations were measured; however, only Cl and Na are discussed in this study. ^{222}Rn activities in groundwater (Table S2) and surface water (Table S1) were determined using a portable radon-in-air monitor (RAD-7, DurrIDGE Co.) following methods described by (Burnett and Dulaiova, 2006) and are expressed in Bq m^{-3} . 0.5 L of sample was collected by bottom-filling a glass flask and ^{222}Rn was subsequently degassed for 5 min into a closed air loop of known volume. Counting times were 1–2 h for surface water and 20 min for groundwater. Typical relative precision is $< 3 \%$ at $10\,000 \text{ Bq m}^{-3}$ and $\sim 10 \%$ at 100 Bq m^{-3} .

Forty four samples of river bed sediments from sites along the Avon River were collected in order to determine ^{222}Rn production in the hyporheic and parafluvial zones and to further constrain groundwater ^{222}Rn activities. ^{222}Rn emanation rates (γ in $\text{Bq m}^{-3} \text{ day}^{-1}$) (Table 2) were calculated by sealing a known dry weight of sediment in airtight containers with water and allowing ^{222}Rn to accumulate. Following 4–5 weeks incubation, by which time the rate of ^{222}Rn production and decay will have reached steady state, 20 to 40 mL of pore water was extracted and analysed for ^{222}Rn activities

9216

inflows. This section of the Avon River is incised up to 4 m below the floodplain which likely produces steep hydraulic head gradients that will result in groundwater discharge on the floodplain and into the river. There are also groundwater seeps and patches of perennial wetland vegetation at the edge of the floodplain in this area. In February 2009 and April 2010, the highest ^{222}Rn activities were recorded at Pearces Lane, while in March 2014 and February 2015 the highest ^{222}Rn activities were recorded at Bushy Park (Fig. 4a). The major floods between 2011 and 2013 (Fig. 3a) changed the location of pools and sediment banks on the Avon River probably also changed the locations of groundwater inflow. The reaches between Browns and Wombat Flat and Stewarts Lane and Stratford are also characterised by increasing ^{222}Rn activities and are again interpreted as recording groundwater inflows.

The reaches between Wombat Flat and Smyths Road, Riddleys Lane and Stewarts Lane, and Knobs Reserve and Chinns Bridge show gradual decline in ^{222}Rn activities and little change in Cl concentrations (Fig. 4); these are interpreted as either losing or receiving minor groundwater inflows. In these areas, the landscape is flatter and the river less incised which likely results in lower hydraulic gradients and consequently less groundwater discharge to the river.

5.2 Quantifying groundwater inflows

Groundwater inflows were calculated from the ^{222}Rn activities for February 2015 (Table S1) by solving Eq. (1) using a finite difference approach in a spreadsheet with a spatial discretisation of 10 m; comparisons for subsets of the data indicate that finer-scale discretisation does not significantly change the results. The streamflow at The Channel gauge was used as the initial streamflow and Q was increased after each distance step via Eq. (2). The calculations specified all parameters except l and matched the observed ^{222}Rn activity at the sampling sites by varying l in each reach (Fig. 6a).

For the initial set of calculations, the groundwater ^{222}Rn activity was assumed to be $13\,000\text{ Bq m}^{-3}$, which is consistent both with the measured ^{222}Rn activities in the bores and the calculated ^{222}Rn activities of water in equilibrium with the alluvial sediments.

9221

Average evaporation rates in southeast Australia in February to April are 3×10^{-3} to $5 \times 10^{-3}\text{ m day}^{-1}$ (Bureau of Meteorology, 2015) and a value of $4 \times 10^{-3}\text{ m day}^{-1}$ was adopted. Average river width and depth is 10 and 0.5 m, respectively, upstream of Wombat Flat and 20 and 1 m, respectively, for the rest of the river. The gas transfer coefficient was estimated as 0.3 day^{-1} from the decline in ^{222}Rn activities between Riddleys Lane and Schools Road (Fig. 4a). Assuming that this is a losing stretch of the river, which is consistent with the lack of increase in Cl concentrations (Fig. 4b), the decrease in ^{222}Rn activities will be mainly due to degassing with a small contribution from decay. A value of 0.3 day^{-1} is at the lower end of estimates of Rn gas transfer coefficients (Genereux and Hemond, 1992; Cook et al., 2003, 2006; Cartwright et al., 2011, 2014b; Atkinson et al., 2013; Unland et al., 2013; Yu et al., 2014). However, as the Avon River is dominated by slow-flowing pools, degassing rates are expected to be low.

As there are few processes that increase the EC of water in the hyporheic or parafluvial zones, the water in the river gravels within 1 to 2 m of the river that has high EC values (Fig. 5b) represents groundwater or a mixture of river water and groundwater. Consequently, the width of the hyporheic zone has been assigned as the river width. The thickness of the hyporheic zone is less well known; however, by analogy with rivers elsewhere, it is likely to be a few centimetres thick (Boulton et al., 1998; Hester and Doyle, 2008; Tonina and Buffington, 2011) and a value of 10 cm is initially adopted. The flux of ^{222}Rn from the hyporheic zone was estimated from Eq. (3) using the mean γ value of $2300\text{ Bq m}^{-3}\text{ day}^{-1}$ (Table 2), a porosity of 0.4 (which is appropriate for coarse-grained unconsolidated sediments), and a value for c_{in} that is the ^{222}Rn activity of the river in that reach. The residence time of water within the parafluvial zone is likely to be short (Boulton et al., 1998; Tonina and Buffington, 2011; Zarnetske et al., 2011; Cartwright et al., 2014b), and $t_{\text{h}} = 0.1$ days is assumed here; for $t_{\text{h}} < 1$ day, F_{h} is relatively insensitive to the actual residence times in the hyporheic zone (Lamontagne and Cook, 2007; Cartwright et al., 2014b)

Using these parameters it is possible to model the observed ^{222}Rn activities in the Avon River in February 2015 (Fig. 6a). Calculated groundwater inflows are up to $2.7\text{ m}^3\text{ m}^{-1}\text{ day}^{-1}$ in the reaches between Smyths Road and Pearces Lane (Fig. 6b), which is the region where Cl concentrations also increase markedly (Fig. 4b). Most reaches of the river between Ridleys Lane and Stewarts Lane and downstream of Knobs Reserve have negligible groundwater inflows or are losing (Fig. 6b). The change in Cl concentrations (Fig. 6d) was calculated from the groundwater inflows assuming that groundwater has a Cl concentration of 85 mg L^{-1} . The calculated Cl concentrations are higher than observed, although the calculations do predict the marked increase in Cl concentrations between Smyths Road and Ridleys Lane. Given the uncertainty in groundwater Cl concentrations, the discrepancy between observed and predicted Cl concentrations is not large. If the Cl concentration of the groundwater is allowed to vary by the 95% confidence interval ($\pm 16\text{ mg L}^{-1}$) the observed trend can be reproduced (Fig. 6d).

The calculated net groundwater inflow of $28\,300\text{ m}^3\text{ day}^{-1}$, however, exceeds the measured increase in streamflow between The Channel and Chinns Bridge of $15\,500\text{ m}^3\text{ day}^{-1}$ by 180% (Fig. 6c). Much of the mismatch between observed and calculated streamflow results from the high estimates of groundwater inflows upstream of Stratford (Fig. 6b). The net increase in streamflow between The Channel and Stratford in February 2015 is $10\,500\text{ m}^3\text{ day}^{-1}$, whereas the predicted net groundwater inflow from the ^{222}Rn mass balance was $26\,700\text{ m}^3\text{ day}^{-1}$. While the February 2015 sampling round represents the end of summer when the small ephemeral tributaries were dry and there was no overland flow, there were still flows from Valencia Creek and Freestone Creek of 1410 and $200\text{ m}^3\text{ day}^{-1}$, respectively. If these were included, the mismatch between calculated and observed streamflow increases.

Although constrained by fewer data points, the predicted distribution of groundwater inflows in the other low to moderate flow sampling campaigns calculated using the same parameters as for February 2015 are similar (Fig. 7a). In February 2009, April 2010, and March 2014, groundwater inflows are up to $3.1\text{ m}^3\text{ m}^{-1}\text{ day}^{-1}$ and the

9223

calculated net groundwater inflows are $21\,700$, $15\,900$, and $21\,300\text{ m}^3\text{ day}^{-1}$, respectively (Fig. 7b). These calculated groundwater inflows are up to 490% of the measured increases in streamflow between The Channel and Chinns Bridge. Groundwater inflows were also calculated for the higher streamflow sampling rounds (September 2010 and July 2014) using widths of 15 m upstream of Wombat Flat and 25 m elsewhere, depths of 1.25 m upstream of Wombat Flat and 1.6 m elsewhere, $k = 0.3\text{ day}^{-1}$, and F_h adjusted for the higher river widths. The estimated groundwater inflows are lower (up to $1.3\text{ m}^3\text{ m}^{-1}\text{ day}^{-1}$) than at the periods of low streamflow and the net groundwater discharges of $32\,100\text{ m}^3\text{ day}^{-1}$ in September 2010 and $44\,600\text{ m}^3\text{ day}^{-1}$ in July 2014 are lower than the measured increases in streamflow between The Channel and Stratford or Chinns Bridge (Fig. 7b).

5.3 Uncertainties and variability

The impacts of uncertainties need in the parameters in Eq. (1) on the calculated groundwater inflows need to be considered. This will be done in reference to the February 2015 sampling round but the same considerations apply to the other sampling rounds. The evaporation term in Eq. (1) is one to two orders of magnitude lower than most of the other terms and errors in the assumed evaporation rate have little influence on the calculations (Cook, 2013). The main factor impacting calculated groundwater inflows in reaches where groundwater inflows are high is the assumed ^{222}Rn activity of groundwater (Cartwright et al., 2011; Cook, 2013). Allowing c_{gw} to vary by $\pm 2600\text{ Bq m}^{-3}$, which represents the 95% confidence interval of the groundwater ^{222}Rn activities, makes little difference to the discrepancy between the calculated and observed increase in streamflow (Fig. 6c). Increasing c_{gw} to $\sim 27\,000\text{ Bq m}^{-3}$ would reproduce the observed increase in streamflow along the Avon (Fig. 8). However, there is no known groundwater in the Avon catchment with such high ^{222}Rn activities, and an activity of $27\,000\text{ Bq m}^{-3}$ is far higher than would be in equilibrium with the alluvial

9224

5.4 Incorporating larger-scale parafluvial flow

It is clear that it is difficult to find combinations of parameters that allow the observed variation in ^{222}Rn activities to be replicated without the calculated net groundwater inflows exceeding the measured increase in streamflow. The proposed resolution is that there is large-scale (100's of m to km) parafluvial flow through the alluvial sediments on the Avon River floodplain that contributes to the river in the gaining reaches. This flow represents water that exfiltrates from and then re-infiltrates into the river which is likely hosted mainly within the coarse-grained alluvial sediments (although conceivably it could also include water that flows through the upper levels of the aquifers underlying the alluvial sediments). By contrast with hyporheic flow which contributes ^{222}Rn to the river along all reaches (whether gaining or losing), the inflows from the parafluvial zone will only contribute ^{222}Rn where the river is gaining.

If residence times of water in the parafluvial zone are sufficiently long, then the inflowing parafluvial water will have high ^{222}Rn activities and increase the ^{222}Rn activities in the river. However, because it represents exfiltrated river water, the inflows from the parafluvial zone do not add to the overall streamflow. Figure 10 shows the results of assuming that 50% of the water inflowing in each reach in February 2015 represents parafluvial zone waters that has a residence time in the parafluvial zone sufficiently long for secular equilibrium to be attained. The maximum value of I_p is $1.26 \text{ m}^3 \text{ m}^{-1} \text{ day}^{-1}$ (Fig. 10b) in the Valencia to Bushy Park reaches where c_r is 2500 to 2900 Bq m^{-3} . If the parafluvial zone water is in secular equilibrium with the sediments, $c_p \sim 12\,700 \text{ Bq m}^{-3}$ (Table 2), $c_p - c_r \sim 10\,000 \text{ Bq m}^{-3}$, and $F_p \sim 12\,600 \text{ Bq m}^{-1} \text{ day}^{-1}$ (Eq. 5). For t_p in excess of ~ 30 days the system is close to secular equilibrium and c_p and I_p are near constant and independent of t_p (Fig. 1). If residence times in the parafluvial zone are shorter than those required to attain secular equilibrium, c_p will be lower and the inflows from the parafluvial zone (I_p) required to produce a given flux of ^{222}Rn (F_p) increases (Fig. 1). For example, if $\gamma = 2300 \text{ Bq m}^{-3} \text{ day}^{-1}$, $c_r = 2700 \text{ Bq m}^{-3}$, and $t_p = 0.1$ days,

$$9227$$

$c_p = 2718 \text{ Bq m}^{-3}$ and if $F_p = 12\,600 \text{ Bq m}^{-1} \text{ day}^{-1}$, $I_p \sim 70 \text{ m}^3 \text{ m}^{-1} \text{ day}^{-1}$. The cross-sectional area of the parafluvial zone A_p required to accommodate these parafluvial flows with $\phi = 0.4$ and t_p between 0.1 and 100 days is between 17 and 350 m^2 (Eq. 6). The floodplain of the Avon River is tens of metres wide with sediment thicknesses of several metres and even the higher estimates of the cross-sectional area are not unreasonable. For the lower estimates of A_p , the flow could be accommodated in a zone < 1 m thick beneath the river.

The proposal that inflows of parafluvial zone waters augment groundwater inflows is justifiable hydrologically as the conditions required for high groundwater inflows (gaining river with steep hydraulic gradients and high-hydraulic conductivity sediments) will likely drive the return of parafluvial waters to the river. By contrast losing reaches are likely to be where the water enters the parafluvial sediments. The riffle sections of the Avon River commonly have steep longitudinal gradients and may transition from losing at their upstream end to gaining at the downstream end. Additionally, there may be parafluvial flow through the numerous sediment banks and point bars.

By allowing the parafluvial input to vary between reaches, both the variations in ^{222}Rn activities (Fig. 10a) and calculated increases in streamflow are predicted (Fig. 10c). There is no process in the parafluvial zone that increases the Cl concentrations of the through-flowing water. Thus the Cl concentrations in the river reflect only the groundwater inflows. The calculated Cl concentrations are again higher than observed (Fig. 10d) but not substantially when the uncertainty in groundwater Cl concentrations is taken into account.

While the model of parafluvial zone flow explains the geochemical observations and is consistent with the hydrogeology of the Avon River, it is difficult to test. The inflows from the parafluvial zone have been assumed to vary proportionally to the groundwater inflows, which may not necessarily be the case. Nevertheless, this conceptualisation utilises a process that is known to occur in river valleys to explain observations that are otherwise difficult to resolve. An alternative explanation for the discrepancy between the calculated inflows and the increase in streamflow is that significant pumping of water

References

- Aksoy, H., Kurt, I., and Eris, E.: Filtered smoothed minima baseflow separation method, *J. Hydrol.*, 372, 94–101, 2009.
- Atkinson, A., Cartwright, I., Gilfedder, B., Hofmann, H., Unland, N., Cendón, D., and Chisari, R.: A multi-tracer approach to quantifying groundwater inflows to an upland river; assessing the influence of variable groundwater chemistry, *Hydrol. Process.*, 29, 1–12, 2015.
- Barron, O., Silberstein, R., Ali, R., Donohue, R., McFarlane, D. J., Davies, P., Hodgson, G., Smart, N., and Donn, M.: Climate change effects on water-dependent ecosystems in south-western Australia, *J. Hydrol.*, 434–435, 95–109, 2012.
- Boulton, A. J., Findlay, S., Marmonier, P., Stanley, E. H., and Maurice Valett, H.: The functional significance of the hyporheic zone in streams and rivers, *Annu. Rev. Ecol. Syst.*, 29, 59–81, 1998.
- Bourke, S. A., Cook, P. G., Shanafield, M., Dogramaci, S., and Clark, J. F.: Characterisation of hyporheic exchange in a losing stream using radon-222, *J. Hydrol.*, 519, 94–105, 2014a.
- Bourke, S. A., Harrington, G. A., Cook, P. G., Post, V. E., and Dogramaci, S.: Carbon-14 in streams as a tracer of discharging groundwater, *J. Hydrol.*, 519, 117–130, 2014b.
- Brodie, R., Sundaram, B., Tottenham, R., Hostetler, S., and Ransley, T.: An Overview of Tools for Assessing Groundwater-Surface Water Connectivity, Bureau of Rural Sciences, Canberra, Australia, 133 pp., 2007.
- Brumley, J.: An investigation of the groundwater resources of the Latrobe Valley, Victoria, *Proc. Geol. Soc. Austr. Coal Group Symposium*, Sydney, Australia, 562–581, 1982.
- Bureau of Meteorology: Commonwealth of Australia Bureau of Meteorology, available at: <http://www.bom.gov.au>, last access: 30 June 2015.
- Burnett, W. C. and Dulaiova, H.: Radon as a tracer of submarine groundwater discharge into a boat basin in Donnalucata, Sicily, *Cont. Shelf Res.*, 26, 862–873, 2006.
- Cartwright, I. and Gilfedder, B.: Mapping and quantifying groundwater inflows to Deep Creek (Maribyrnong catchment, SE Australia) using ^{222}Rn , implications for protecting groundwater-dependant ecosystems, *Appl. Geochem.*, 52, 118–129, 2015.
- Cartwright, I., Hofmann, H., Sirianos, M. A., Weaver, T. R., and Simmons, C. T.: Geochemical and ^{222}Rn constraints on baseflow to the Murray River, Australia, and timescales for the decay of low-salinity groundwater lenses, *J. Hydrol.*, 405, 333–343, 2011.

9231

- Cartwright, I., Gilfedder, B., and Hofmann, H.: Contrasts between estimates of baseflow help discern multiple sources of water contributing to rivers, *Hydrol. Earth Syst. Sci.*, 18, 15–30, doi:10.5194/hess-18-15-2014, 2014a.
- Cartwright, I., Hofmann, H., Gilfedder, B., and Smyth, B.: Understanding parafluvial exchange and degassing to better quantify groundwater inflows using ^{222}Rn : the King River, southeast Australia, *Chem. Geol.*, 380, 48–60, 2014b.
- Cecil, L. D. and Green, J. R.: Radon-222, in: *Environmental Tracers in Subsurface Hydrology*, edited by: Cook, P. G. and Herczeg, A. L., Kluwer, Boston, USA, 175–194, 2000.
- Cochrane, G. W., Quick, G. W., and Spencer-Jones, D.: *Introducing Victorian Geology*, Geological Society of Australia, Victorian Division, Melbourne, Australia, 304 pp., 1991.
- Cook, P. G.: Estimating groundwater discharge to rivers from river chemistry surveys, *Hydrol. Process.*, 27, 3694–3707, 2013.
- Cook, P. G., Favreau, G., Dighton, J. C., and Tickell, S.: Determining natural groundwater influx to a tropical river using radon, chlorofluorocarbons and ionic environmental tracers, *J. Hydrol.*, 277, 74–88, 2003.
- Cook, P. G., Lamontagne, S., Berhane, D., and Clarke, J. F.: Quantifying groundwater discharge to Cockburn River, southeastern Australia, using dissolved gas tracers Rn-222 and SF₆, *Water Resour. Res.*, 42, W10411, doi:10.1029/2006WR004921, 2006.
- Department of Environment and Primary Industries: Victoria Department of Environment and Primary Industries Water Monitoring, available at: <http://data.water.vic.gov.au/monitoring.htm>, last access: 10 July 2015.
- Edwardson, K. J., Bowden, W. B., Dahm, C., and Morrice, J.: The hydraulic characteristics and geochemistry of hyporheic and parafluvial zones in Arctic tundra streams, north slope, Alaska, *Adv. Water Resour.*, 26, 907–923, 2003.
- Ellins, K. K., Roman-Mas, A., and Lee, R.: Using ^{222}Rn to examine groundwater/surface discharge interaction in the Rio Grande de Manati, Puerto Rico, *J. Hydrol.*, 115, 319–341, 1990.
- Freeze, R. A. and Cherry, J. A.: *Groundwater*, Prentice-Hall, New Jersey, USA, 604 pp., 1979.
- Geneux, D. P. and Hemond, H. F.: Determination of gas exchange rate constants for a small stream on Walker Branch watershed, Tennessee, *Water Resour. Res.*, 28, 2365–2374, 1992.
- Gippsland Water: Water Supply Demand Strategy, available at: <http://www.gippswater.com.au/>, 2012, last access: 30 May 2015.
- Hester, E. T. and Doyle, M. W.: In-stream geomorphic structures as drivers of hyporheic exchange, *Water Resour. Res.*, 44, W03417, doi:10.1029/2006WR005810, 2008.

9232

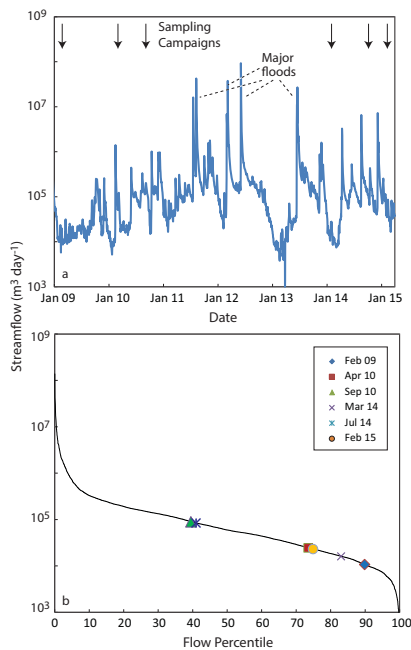


Figure 3. (a) Variation in streamflow at Stratford (Fig. 1) between January 2009 and March 2015. The major floods (highlighted) caused significant changes to the geometry of the floodplain. (b) Flow frequency curve for Stratford for streamflows between January 2000 and March 2015 and the percentiles of discharge in the sampling campaigns. Data from Department of Environment and Primary Industries (2015).

9239

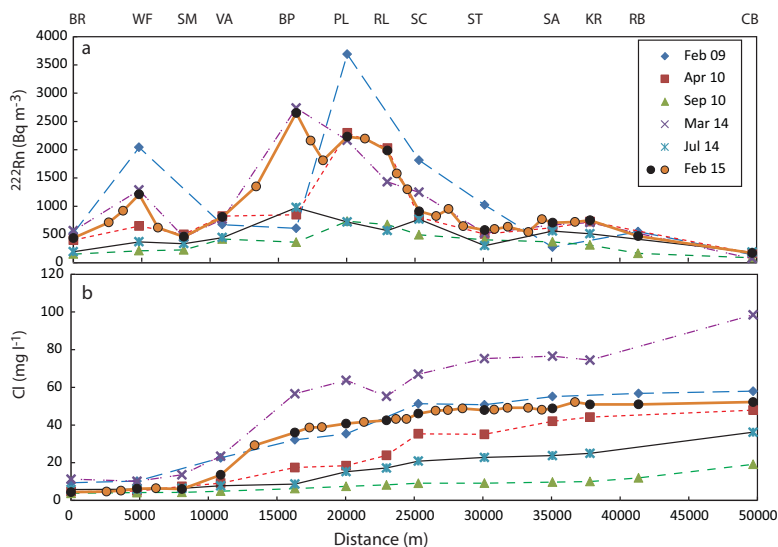


Figure 4. Downstream variations in ^{222}Rn activities (a) and Cl concentrations (b) for the six sampling campaigns (Data from Table S1, abbreviations as for Fig. 2). Closed symbols for February 2015 are from the main sites, open symbols are from the additional sites specific to that sampling campaign (Table S1). Site abbreviations as for Fig. 2.

9240

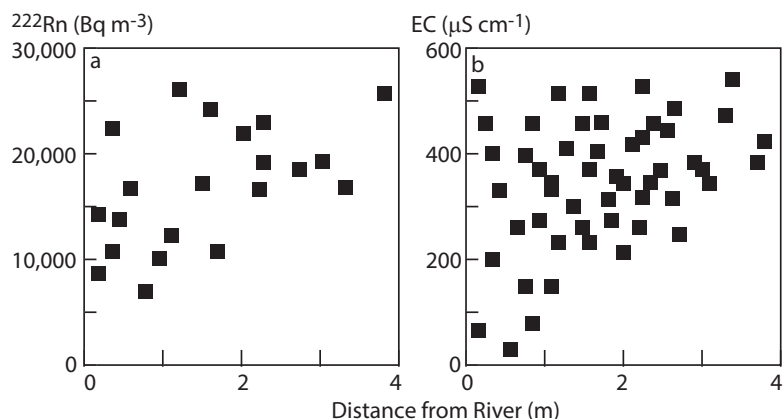


Figure 5. (a) Variations in ^{222}Rn activities (a) and EC values (b) of water extracted from river bank gravels.

9241

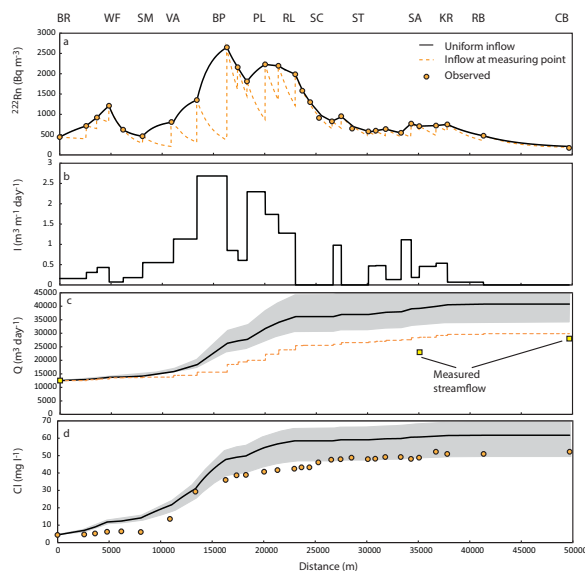


Figure 6. (a) Calculated vs. observed ^{222}Rn activities in the Avon River for February 2015 assuming both uniform groundwater inflow within each reach and the situation where groundwater inflow occurs immediately upstream of the measurement point. Site abbreviations as for Fig. 2. (b) Calculated groundwater inflows (I) assuming uniform inflows within each reach. (c) Calculated increase in streamflow from groundwater inflows (Eq. 2). Both uniform groundwater inflow within each reach and the situation where groundwater enters the river immediately upstream of the measurement point overestimate the measured streamflow. Shaded area is the range of streamflow resulting from varying c_{gw} within the 95 % confidence interval. (d) Predicted vs. observed Cl concentrations. Shaded field is the range resulting from varying groundwater Cl concentrations within the 95 % confidence interval.

9242

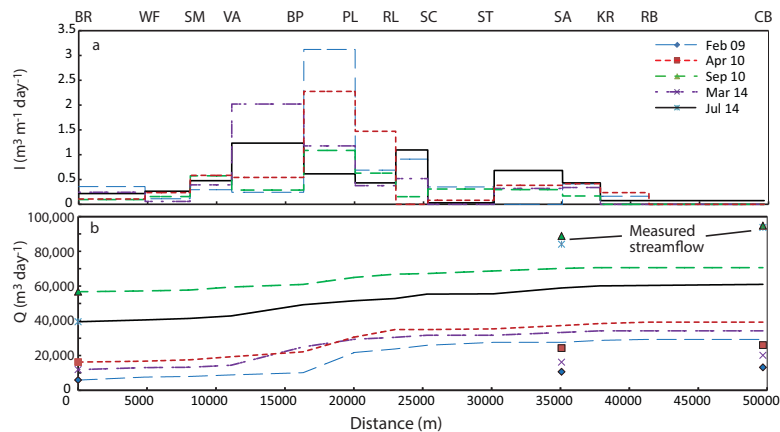


Figure 7. Calculated groundwater inflows (a) and increases in streamflow due to groundwater inflows (b) for the sampling rounds excluding February 2015. Aside from the high flow periods (September 2010 and July 2014) the calculated increase in streamflow exceeds the observed streamflow at Stratford and Chinn's Bridge. Site abbreviations as for Fig. 2.

9243

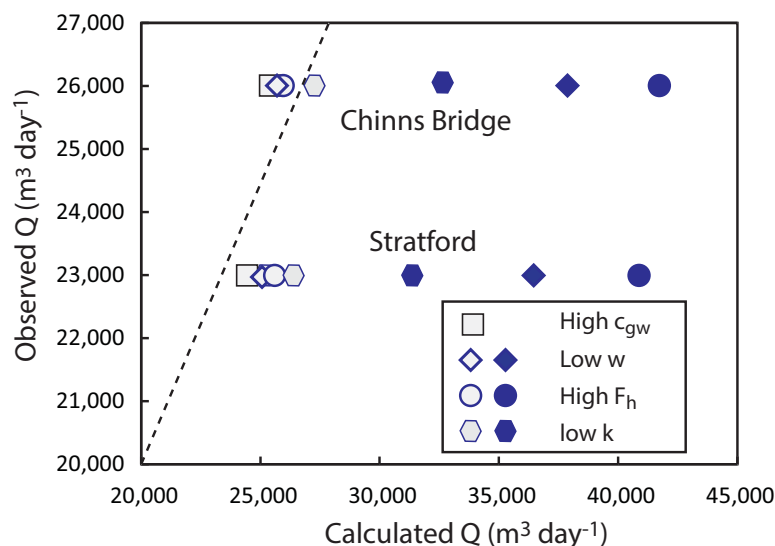


Figure 8. Calculated vs. observed streamflow at Stratford and Chinn's Bridge for February 2015 resulting from varying parameters in Eq. (1). High c_{gw} is for a groundwater ^{222}Rn activity of $27\,000\text{ Bq m}^{-3}$; low k is where k is reduced to 0.1 day^{-1} , high F_h increase the thickness of the parafluvial zone to 0.5 m , and low w reduces the width of the Avon River by 50% . Open symbols represent the result of these changes in isolation (see also Fig. 9); closed symbols represent the results of varying other parameters so that the predicted and observed ^{222}Rn activities match.

9244

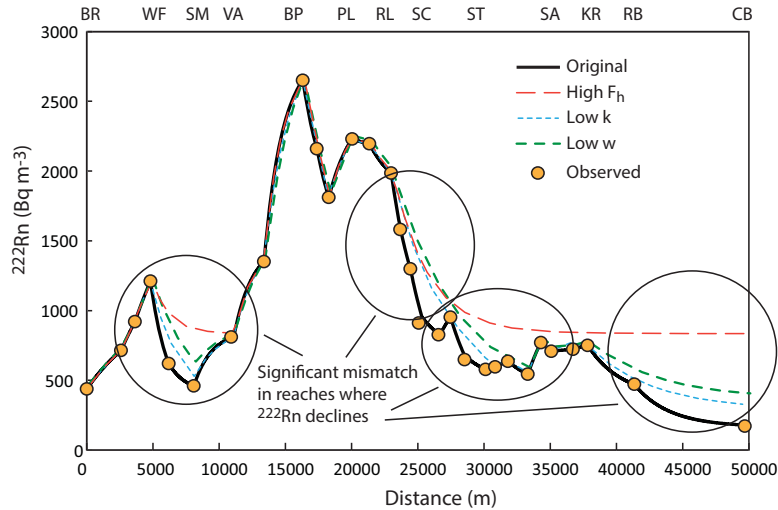


Figure 9. Calculated and observed ^{222}Rn activities for February 2015 resulting from varying individual parameters in Eq. (1) in isolation. Original is the predicted variation in ^{222}Rn activities from Fig. 5, low k is where k is reduced to 0.1 day^{-1} , high F_h increase the thickness of the parafluvial zone to 0.5 m , and low w reduces the width of the Avon River by 50% . In all cases the new parameters result in significant overestimation of ^{222}Rn activities in many reaches and are unlikely to be realistic. Site abbreviations as for Fig. 2.

9245

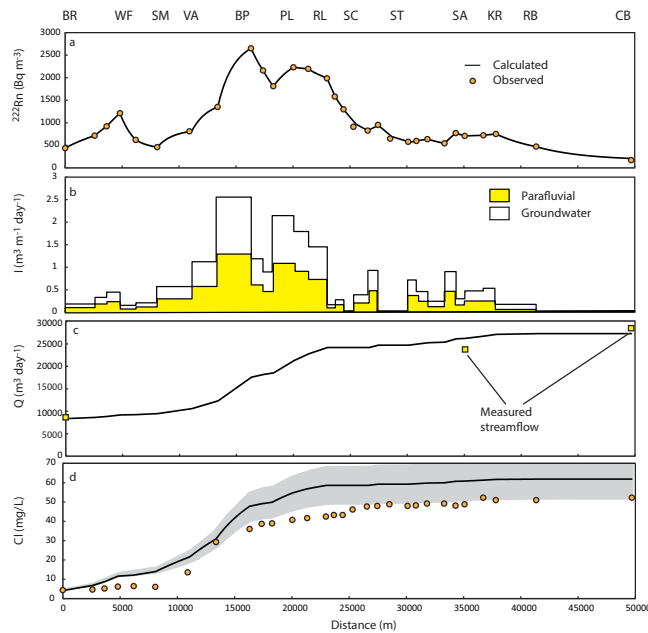


Figure 10. (a) Calculated and observed ^{222}Rn activities for February 2015 resulting from assigning 50% of the calculated inflows as parafluvial flow. (b) Variation in groundwater and parafluvial inflows. (c) Calculated streamflow resulting from the groundwater inflows (Eq. 2) vs. measured streamflow at Stratford and Chinns Bridge. (d) Predicted vs. observed Cl concentrations. Shaded field is the range resulting from varying groundwater Cl concentrations within the 95% confidence interval.

9246